School of Pharmaceutical Sciences[1], Shandong University; Shandong Cancer Hospital Affiliated to Shandong University[2]; Shandong Institute of Commerce & Technology[3], Jinan, China

Protective effects and possible molecular mechanism of *Hovenia dulcis* Thunb. extract on acetaminophen-induced hepatotoxicity

Sijing Dong[1], Jianbo Ji[1], Baofang Zhang[1], Lingyun Hu[2], Xiangzhen Cui[3], Haina Wang[1,*]

Received July 17, 2018, accepted August 24, 2018

**Corresponding author: Dr. Haina Wang, School of Pharmaceutical Sciences, Shandong University, Jinan 250012, China*
whn2013@sdu.edu.cn

Pharmazie 73: 666–670 (2018) *doi: 10.1691/ph.2018.8650*

Hovenia dulcis Thunb. is a traditional hepatoprotective Chinese medicine, and in research, much effort has been focused on the protection against alcoholic liver injury. In this study, the protective effects of a fruit ethanol extract of *Hovenia dulcis* (FE) against APAP-induced acute hepatotoxicity in mice and the possibly involved molecular mechanisms were investigated. Hepatoprotective activity of FE is clearly indicated by histopathological and biochemical examination. Treatment with FE resulted in inhibition of CYP2E1 activity involved in the transformation of APAP *in vivo*. Expressions of the altered bile acid metabolism and transport-related genes and relative proteins of apoptosis were normalized by preconditioning with FE before APAP treatment. These results suggested FE to alleviate APAP-induced liver injury in a dose-dependent manner by inhibition of cytochrome P450 activity, hepatocyte apoptosis and regulation of bile acid homeostasis imbalance.

1. Introduction

Hovenia dulcis, known as Japanese raisin tree, has usually been found in East Asia (especially Japan, China and South Korea) but was introduced as an ornamental plant to other areas later. Its leaves, seeds, fruits, roots, and bark are used as traditional herbal (Hyun et al. 2010). *Hovenia dulcis* Thunb., whos dried ripe fruits are also known as Japanese grape, is a member of family *Hovenia* (Rhamnaceae) (Maieves et al. 2015). Reported medicinal values of *Hovenia dulcis* Thunb. extract include accelerated detoxification of ethanol, and hepatoprotective, anti-oxidative, and anti-diabetic properties. Its role in liver protection and alcoholism has been discussed (Chen et al. 2003; Hyun et al. 2010).

Acetaminophen (APAP) is a widely used analgesic and antipyretic agent with few side effects if taken in reasonable doses (Jiang et al. 2015). However, APAP can cause serious hepatotoxicity in high doses or long-term use and is regarded as a common cause of acute liver failure (Yan et al. 2016; Choi et al. 2017). Meanwhile, liver injury caused by APAP has become a useful model in studies of hepatoprotective agents (Xie et al. 2016a; Choi et al. 2017).

Numerous efforts have been undertaken to explain the molecular mechanism of APAP toxicity (Lee et al. 2016; Xie et al. 2016b). Briefly, under safe dosage, more than 80-90% of an administered dose of APAP is conjugated with glucuronic acid or sulfate and excreted. APAP is oxidized by cytochrome P450 enzymes including CYP1A2, CYP2E1 to its chemically reactive metabolite N-acetyl-p-benzoquinoneimine (NAPQI) which can cause liver injury when APAP is overdosed (Chen et al. 2003). NAPQI accumulation will result in increased utilization of GSH and depletion of GSH stores. Coupling of NAPQI, cellular proteins, glutathione (GSH) depletion and oxidative stress may trigger signaling pathways through mitochondrial toxicity later, finally resulting in fatal cell necrosis and liver damage (Jiang et al. 2015; Huo et al. 2017; Reshi et al. 2017).

In a previous study, research on the hepatoprotective effect of *Hovenia dulcis* Thunb. mainly focused on the protection against alcoholic liver injury (Du et al. 2010). Taking into account that APAP overdose frequently results in serious hepatotoxicity, this study explores the potential ameliorative effect of fruit ethanol extract of *Hovenia dulcis* Thunb. (FE) in a mouse model of APAP-induced liver hepatotoxicity. The protective mechanism of FE against APAP-induced liver injury is revealed for the first time.

2. Investigations and results

2.1. FE Characterization

The main constituents of FE were analyzed by HPLC separation. The HPLC-DAD analysis showed two major compounds, quercetin and dihydromyricetin, which were identified at 14.53 and 33.46 min, respectively (Fig. 1). These compounds were identified by standards dihydromyricetin ($C_{15}H_{12}O_8$, >98.0% HPLC grade) and quercetin ($C_{15}H_{10}O_7$, >98.0% HPLC grade) compounds. The preparation of standard calibration curves was used for qualification of every compound. Dihydromyricetin and quercetin standard curves were y=3155.5x-4.1225 (R^2=0.9962) and y=12.852x+278.94 (R^2=0.9961). The content of dihydromyricetin and quercetin was quantified as 414.9±0.016 μg/mL and 16.75±3.65 μg/mL respectively.

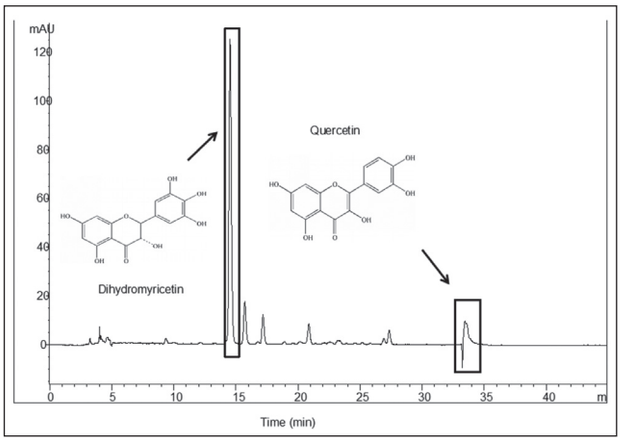

Fig. 1: HPLC-DAD Chromatogram of FE

2.2. Effect of FE on body weight and gallbladder

The weight changes of mice are shown in Fig. 2a. Final weight of APAP groups displayed significant ($p<0.001$) decrease compared with other groups, and the A+FE200, A+FE400, A+FE800 groups

showed both normal values, which means that FE might relieve the damage caused by APAP. Moreover, there was significant gallbladder enlargement in the APAP group (Fig. 2b). The appropriate dose of FE pretreatment could alleviate this phenomenon to some extent.

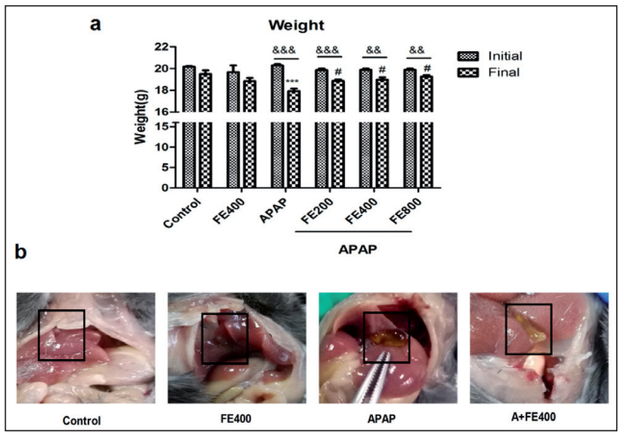

Fig. 2: Effects of FE on body weights and gallbladders (n=6) a, body weights. b, gallbladders of Control, FE400, APAP and A+FE400 groups. ***p<0.001 compared with the control group final weight, #P<0.05 compared with the APAP group final weight. &&P<0.01, &&&P<0.001 compared with the initial weight.

2.3. *Effect of FE on APAP-induced histopathological alterations*

Liver sections from four groups (Control, FE400, APAP, A+FE400) were examined by H&E or Hoechst 33258 staining; results are shown in Fig. 3a and b. For H&E staining, the perivascular liver cells showed focal coagulation necrosis in APAP groups. For Hoechst 33258 staining, the high density of blue apoptotic liver cells and small chunks of nuclei indicated hepatocyte apoptosis obviously caused by APAP treatment. Preconditioning with FE resulted in an improvement in APAP-induced liver damage and apoptosis.

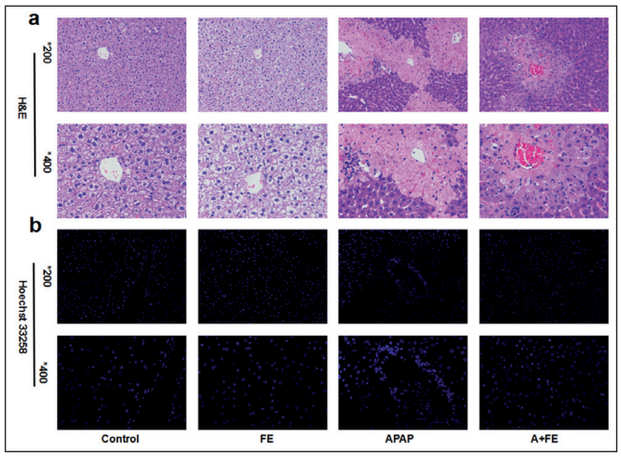

Fig. 3: Representation of histopathological abnormalities (n=3) a and b, liver tissues stained with H&E or Hoechst 33258 on Control, FE400, APAP and A+FE400 groups.

2.4. *Effect of FE on APAP-induced liver damage*

Elevation of the serum marker enzymes ALT, AST, LDH caused by APAP were significantly decreased (p<0.05) when 400 mg/kg or 800 mg/kg FE were administered (Fig. 4a), which means that the administration of FE (400 mg/kg or 800 mg/kg) could protect from hepatotoxicity caused by APAP. In addition, pretreatment with FE (400 mg/kg or 800 mg/kg) could significantly reduce the increase of many lipid indicators caused by APAP (p<0.05) which is indicated in Fig. 4a.

2.5. *Effect of FE on APAP-induced oxidative stress attenuation*

Oxidative stress seems to be an important pathogenic factor in APAP-induced hepatotoxicity (Liu et al. 2010). As mentioned in previously, high concentrations of APAP might cause GSH depletion in the liver, affect liver functions and lead to massive hepatocyte necrosis, liver failure or death (Ramachandran and Jaeschke 2017). There is also evidence of APAP-induced liver injury via an oxidative stress mechanism caused by increased MDA and reduced GSH levels (Ding et al. 2016; Shanmugam et al. 2016; Yoshioka et al. 2017). The results presented in Fig. 4b show that the levels of AKP, MDA were elevated significantly (p<0.05) in the APAP treated mice, the level of GSH and SOD were decreased markedly at the same time. Meanwhile, pretreatment with 400 or 800 mg/kg of FE could reduce the degree of liver oxidation caused by APAP which was indicated by the level of MDA and SOD. In addition, the concentrations of GSH in A+FE400 and A+FE800 groups were significantly higher than those in the APAP model group, suggesting that the hepatoprotective mechanism of the drug may be related to its effects on the metabolism of APAP *in vivo*.

2.6. *Effect of FE on bile acid metabolism and transportation*

The rate-limiting enzymes CYP7A1, CYP8B1 and CYP27A1 play an important role in bile acid synthesis and homeostasis (Yang et al. 2016). CYP7A1, CYP8B1 and CYP27A1 mRNAs were found to be increased (P<0.05) in the A+FE400 group compared with the APAP group (Fig. 5a). Multidrug resistance-related protein 2 (MRP2), bile salt export pump (BSEP) export bile acids into canaliculi (Tan et al. 2016). Bsep and Mrp2 mRNAs returned to normal by FE pretreatment (Fig. 5b). The basolateral transporters such as organic anion-transporting polypeptide 1 (OATP1), organic anion-transporting polypeptide 2 (OATP2) and sodium taurocholate-cotransporting polypeptide (NTCP) are associated with the bile acid uptake (Tan et al. 2016). Oatp1 and Oatp 2 mRNAs decreased in APAP model group and was resumed by pretreatment with FE (Fig. 5c).

2.7. *Effect of FE on APAP metabolic activation*

Activation of APAP *in vivo* begins with CYP enzyme-mediated bioconversion (Chen et al. 2003). The effect of FE on the protein expression of CYP2E1, CYP1A2 was determined by Western blot (Fig. 6a). The Western blot assessment clearly demonstrated that the activity of CYP2E1 was markedly inhibited by FE. However, CYP1A2 activity did not change significantly.

2.8. *Effect of FE on hepatocyte apoptosis*

Based on the liver histopathological results (Fig. 3b), western blot analysis was used to explore the impact of FE on the protein expression levels of caspase-3 caspase-9, cytochrome c, Bax and Bcl-2 in order to test the extent of apoptosis in liver tissues. As depicted in Fig. 6b, pretreatment with FE could reduce the expression level of caspase-3, caspse-9 and cytochrome c compared with APAP alone. In addition, FE pretreatment before APAP administration could significantly upregulate Bcl-2/Bax expression, which indicated that the anti-apoptotic effect of FE is related to the regulation of the Bcl-2 family. The results above demonstrated that FE pretreatment might alleviate APAP-induced hepatocyte apoptosis.

3. Discussion

APAP has been widely used for more than 50 years as an antipyretic and analgesic drug. However, it can produce fatal liver

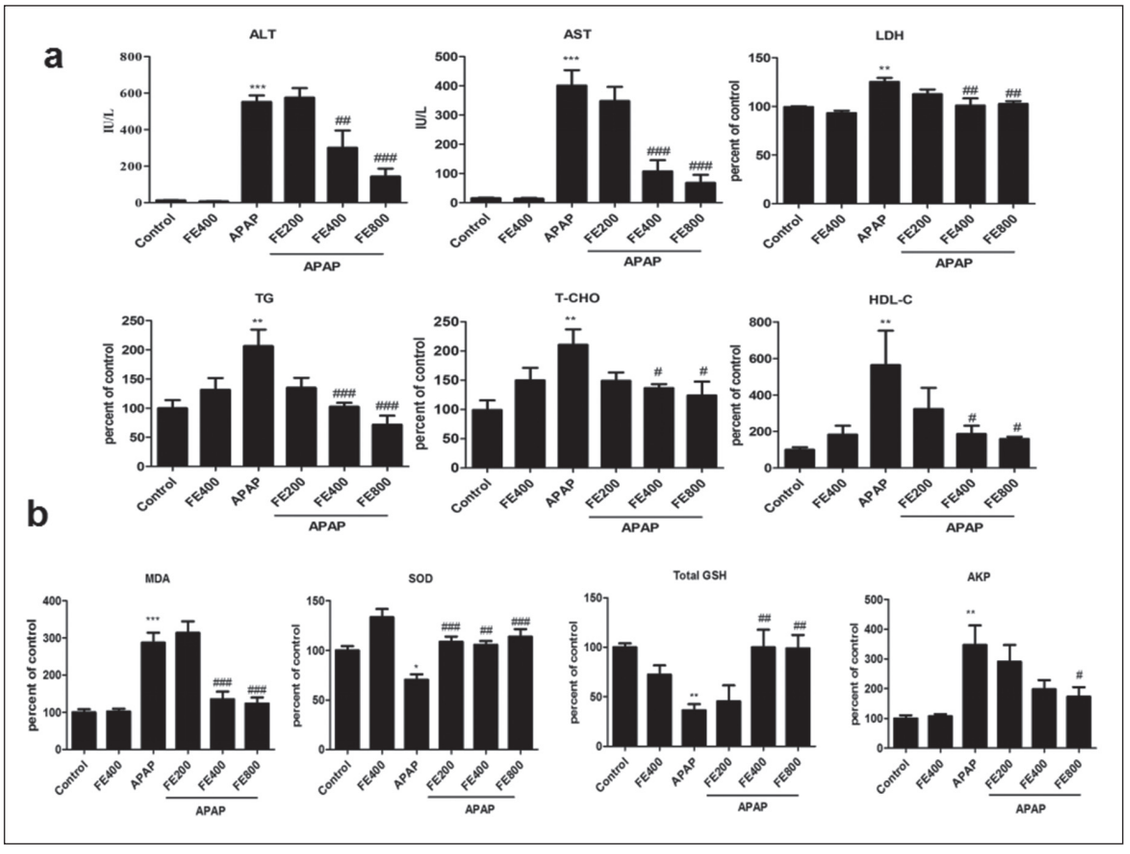

Fig. 4: Representation of altered biochemical parameters (n=6) a and b, analysis of some serum and liver biomarkers in each groups. *P<0.05, **P<0.01, ***P<0.001 compared with the control group, #P<0.05, ##P<0.01, ###P<0.001 compared with the APAP group.

damage (Larson et al. 2005; Amar and Schiff 2007). In the absence of reliable liver protective drugs in modern medical practice, herbs play an important role in the treatment of hepatic injury. A number of plants such as *Opuntia robusta* and *Opuntia streptacantha* fruits, *Schisandra sphenanthera, Hovenia dulcis* have been reported to exhibit hepatoprotective activity (Hyun et al. 2010; Bi et al. 2013; Gonzalez-Ponce et al. 2016).

Serum ALT, AST are the most sensitive biomarker enzymes used to evaluate of liver injury (Shih et al. 2013; Suke et al. 2018). In this study, we observed a significant increase in serum ALT, AST in the APAP group (Fig. 4a), while FE decreased the serum levels of

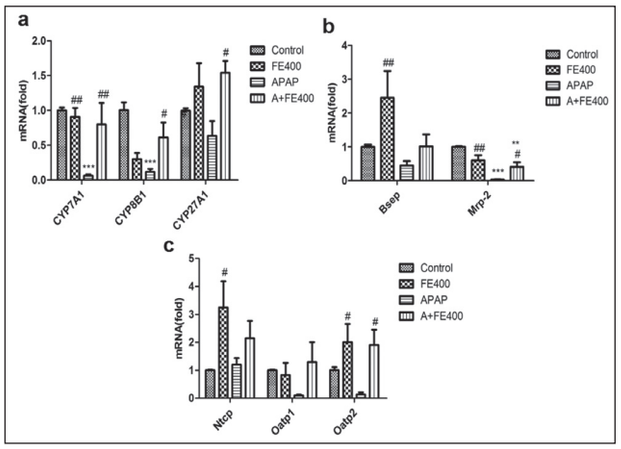

Fig. 5: Effects of FE expression of mRNA on the bile acid genes (n=5) a, the mRNA expressions of bile acid synthesis. b and c, the mRNA expressions of efflux and uptake transporters. *P<0.05, **P<0.01, ***P<0.001 compared with the control group, #P<0.05, ##P<0.01, ###P<0.001 compared with the APAP group.

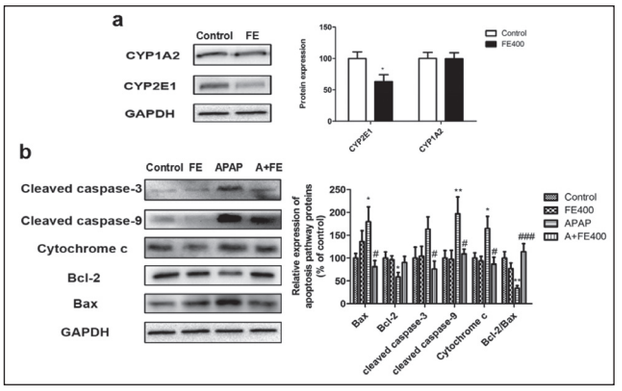

Fig. 6: Western blot analysis of the protein expression involved in APAP biotransformation and apoptisis pathway (n=6) a, expression levels of CYP2E1 and 1A2. b, relative protein levels of Bax, Bcl-2, cleaved caspase-3 and caspase-9, Cytochrome c and Bcl-2/Bax ratio. *P<0.05, **P<0.01, ***P<0.001 compared with the control group, #P<0.05, ##P<0.01, ###P<0.001 compared with the APAP group.

ALT and AST, which indicates a significant protective effect of FE against APAP-induced liver damage in a dose-dependent manner. In addition, we found that some lipid levels in the administration group were significantly lower than those in the APAP group. This suggested that the hepatoprotective effect of FE was likely mediated by altering some of the metabolic pathways of lipids.

Bile acids, the major end-products of cholesterol metabolism, play an important role in the regulation of hepatic lipid, glucose, and energy homeostasis (Wang et al. 2017). Combined with the remission of cholestasis and lipid disorder (Fig. 2b and 4a) caused by APAP after FE pretreatment, we suspected that the protective effect of FE might related to a regulation of bile acid and cholesterol

homeostasis. The experimental results of the gene expression of the bile acid metabolism and transportation confirm this view (Fig. 5).
Because the biological activation of APAP is the main cause of liver toxicity mechanism for APAP, it is important to elucidate whether FE inhibits APAP bioactivation (Jiang et al. 2015; Yuan et al. 2016). Western blotting results showed that FE pretreatment could inhibit the CYP2E1 activity, whereas the CYP1A2 activity was not suppressed (Fig. 6a). On the other hand, the reduction of glutathione consumption after FE pretreatment indicated FE might inhibit the metabolic activation of APAP and result in less GSH depletion indirectly (Fig. 4b). Taken together, the hepatoprotective effect of FE might be exerted through affecting APAP metabolic activation.
Numerous studies have shown that APAP-induced liver injury was associated with liver cell apoptosis, following from release of cytochrome c from the mitochondria, increased Bax, caspase-3, 9 and decreased Bcl-2 activities (Kumari and Kakkar 2012; Wu et al. 2017). In the present paper, the results of western blot analysis showed that pretreatment of FE remarkably decreased Bax, cytochrome c, cleaved caspase-3 and caspase-9 expression and increased Bcl-2 expression compared with APAP alone (Fig. 6b). This might indicate that pretreatment with FE can reduce hepatocyte apoptosis induced by acetaminophen mechanically, which is consistent with the results of Hoechst staining (Fig. 3b).
All in all, our findings clearly demonstrate that FE could dose-dependently protect against APAP-induced hepatotoxicity in mice, potentially through inhibition of APAP bioactivation, regulation of bile acid and lipid homeostasis and reduced apoptosis.

4. Experimental

4.1. Chemicals and reagents

Acetaminophen (purity>99.0%) was purchased from Aladdin Industrial Corporation (Shanghai, China). The kits for the detection of all biochemical assessments were purchased from Nanjing Jiancheng Bioengineering Research Institute (Nanjing, China). The primary antibodies Bax, caspase-3, cytochrome c, Bcl-2 and GAPDH and all secondary antibodies antibody were purchased from Proteintech Group, Inc. (Chicago, USA). The primary antibodies CYP2E1, CYP1A2, Caspase-9 were obtained from Boster Biotechnology (Boster, Wuhan, China).

4.2. Plant material

Fruits of *Hovenia dulcis* were collected in June 2017 in Hunan province (China) and identified by Prof. Lan Xiang, School of Pharmaceutical Sciences, Shandong University (China). The fresh fruits were cleaned, dried under shade and then powdered (77 g) for the following study. After refluxing extraction with 450 mL 75% (v/v) analytical reagent ethanol for 2 h, the filtrate was collected and the reflux process was repeated for the filter residue with 150 mL solvent for 1 h. The mixed decoction was evaporated to dryness under reduced pressure in a rotary evaporator. The extract was freeze-dried and stored at -20 ºC for the evaluation *in vivo*. The yield of FE was 7.9%.

4.3. HPLC-DAD analysis

HPLC analysis was performed on an Agilent 1100 HPLC system (Agilent Technologies, Santa Clara, California, USA) equipped with a Diode Array Detector (DAD). The chromatographic separation was achieved using a Gemini C18 column (4. 6mm × 25 cm, 5 µm). The detection wavelength was set at 340 nm and the column temperature was at 25 ºC. The mobile phase consisted of a mixture of 100% acetonitrile (Solvent A) and 0.1% formic acid (water v/v) (Solvent B). The mobile phase flow rate was 0.8 mL/min with gradient elution. The gradient elution was programmed as follows: 0-23 min 15-23 % A, 23-33 min 23 % A, 33-40 min 23-90 % A. The injection volume was 20 µL. The 15 mg FE powder was dissolved in 10 mL water and acetonitrile (50:50) for HPLC analysis.

4.4. Animal experiments and sample collection

Male C57BL/6 mice (6–8 weeks old, 20±2g) were supplied by the Shandong University Laboratory Animal Center (Shandong, China). The animal room was maintained at 23±1 ºC, 55±5 % humidity with 12 h light/dark cycles. The mice had free access to standard rodent chow and water. All animal study protocols were approved by the Ethics Committee on the Care and Use of Laboratory animals of Shandong University. The hepatoprotective effect of FE was evaluated against the APAP-induced hepatotoxicity following a reported method with slight modifications (Xie et al. 2016a). The animals were weighed and randomly divided into six groups as follows (n=6): (1) Control, (2) APAP (300 mg/kg), (3) FE400 (400 mg/kg), (4) APAP+FE200 (200 mg/kg), (5) APAP+FE400 (400 mg/kg), (6) APAP+FE800 (800 mg/kg). FE was suspended in water for oral administration. Groups 3-6 were gavaged of FE for five consecutive days at doses of 400 mg/kg, 200 mg/kg, 400 mg/kg, 800 mg/kg body weight every day respectively, the normal and APAP groups received water the same way. All mice were fasted for 15 h before intraperitoneal injection. One hour after final treatment, APAP was dissolved in a 0.9% saline and animals except control and FE400 groups received a single intraperitoneal (i.p) injection of APAP (300 mg/kg) to induce acute liver injury. All mice were weighed and killed 9 h after APAP administration and blood and livers were harvested. A small part of the liver was collected in 4 % paraformaldehyde for histology and the remaining tissue was frozen in liquid nitrogen and stored at -80 ºC for further use.

4.5. Histopathological and biochemical examination

Blood was centrifuged at 3000 rpm for 12 min to prepare serum. The supernatant was collected and stored at -20 ºC for the following assay. The liver tissues were homogenized in cold 0.9 % saline and centrifuged at 3000 rpm for 15 min. Liver homogenate protein was measured by bicinchoninic acid (BCA) Protein Assay Kit (Beyotime Biotechnology, Shanghai, China).
Serum alanine aminotransferase (ALT), aspartate transaminase (AST), lactate dehydrogenase (LDH), triglyceride (TG), total cholesterol (T-CHO), high density lipoprotein cholesterol (HDL-C) and liver homogenate glutathione (GSH), malondialdehyde (MDA), superoxide dismutase (SOD), phosphatase (AKP) were determined using Thermo Scientific Multiskan FC Microplate Photometer (Thermo Fisher Scientific,USA).
H&E and Hoechst 33258 stainings were performed as previously described with some modifications (Li et al. 2016). In short, fresh liver tissues fixed in 4% paraformaldehyde were processed with routine embedding and cut to 5 µm thickness. Slides were examined for histological architecture by hematoxylin-eosin (H&E) or Hoechst 33258 staining. Slides were observed for histopathological changes using a light microscope (Leica, Wetzlar, Germany) and fluorescent microscope (Olympus, Tokyo, Japan).

Table: Sequences of the primers used in the Q-PCR in the study

Genes	Forward primers	Reverse primers
CYP7A1	GTCCGGATATTCAAGGATGC	GGGAATGCCATTTACTTGGA
CYP8B1	GATAGGGGAAGAGAGCCACC	TCCTCAGGGTGGTACAGGAG
CYP27A1	GGGCACTAGCCAGATTCACA	CTATGTGCTGCACTTGCCC
Mrp-2	TCTGTGAGTGCAAGAGACAGGT	TCCAGGACCAAGAGATTTGC
Bsep	AAGGACAGCCACACCAACTC	CCAGAACATGACAAACGGAA
Oatp1	TAATCGGGCCAACAATCTTC	ACTCCCATAATGCCCTTGG
Oatp2	TAGCTGAATGAGAGGGCTGC	ACCAAACTCAGCATCCAAGC
Ntcp	TCCGTCGTAGATTCCTTTGC	AGGGGGACATGAACCTCAG
GAPDH	AGGTCGGTGTGAACGGATTTG	GGGGTCGTTGATGGCAACA

4.6. Quantitative-PCR analysis

Total mRNA was extracted from liver tissues by 1 mL TRIzol reagent (Invitrogen, Carlsbad, CA) and determined by NanoDrop (Thermo Scientific, Rockford, IL). Reverse transcription was performed with M-MLV Reverse Transcriptase and complementary DNA (cDNA) was synthesized from 2.5 µg total RNA. The procedure was conducted according to the manufacturer's protocol. All the qPCR primer sequences listed in the Table were reported previously (Tan et al. 2016).
The qPCR reaction was composed of 2.5 µL total cDNA, 1.25 µL forward primer, 1.25 µL reverse primer and 5 µL LightCycle 480 SYBR Green I Master Mix (FastStart Taq DNA polymerase, reaction buffer, dNTP mix, SYBR Green I dye, and $MgCl_2$). All reactions were performed on qTOWER3.0 G Real-Time PCR System (Analytik Jena AG, Jena, Germany). Relative mRNA levels were calculated using GAPDH as the internal control.

4.7. Western blot analysis

The liver samples were homogenized with Radio Immunoprecipitation Assay (RIPA) lysis buffer containing 1 mM phenylmethanesulfonyl fluoride (PMSF) and protein

concentrations were measured by BCA protein assay kit (Beyotime Biotechnology, Shanghai, China). Equal amounts of protein were analyzed by 12 % sodium dodecyl sulfate polyacrylamide gel electropheresis (SDS-PAGE) and transferred onto 0.22 μm polyvinylidene fluoride membrane (BioRad, Germany). Then the membrane was blocked with 5 % non-fat milk in Tris-buffered saline (TBS) containing 0.1%Tween-20 (TBST). After incubating with primary antibodies at 4 ℃ overnight and washing three times with TBST, the membrane was incubated with the secondary antibodies for 1h at room temperature. Ultimately, signals were visualized using electrochemiluminescence (ECL) western blotting detection system (Beyotime Institute of Biotechnology, Haimen, China). And the results were expressed as fold changes normalized to the GAPDH expression.

4.8. Statistical analysis

All data were expressed as means±standard error of means (S.E.) values. The analysis of results was finished using the one-way ANOVA test followed by Dunnett's multiple comparison post hoc test or unpaired Student's test with a confidence level of 95%. GraphPad Prism 5 software was employed to make resulting data chart (GraphPad Software Inc., San Diego, CA).

Acknowledgments: This study was funded by the Key Technologies R & D Program of Shandong Province (No. 2016GSF201003), Shandong Natural Science Foundation of China (No. ZR2017MH030) and the Scientific Research Foundation for the Returned Overseas Chinese Scholars, State Education Ministry (the 50th Batch).

Conflicts of interest: None declared.

References

Amar PJ, Schiff ER (2007) Acetaminophen safety and hepatotoxicity - where do we go from here? Expert Opin Drug Saf 6: 341-355.

Bi HC, Li F, Krausz KW, Qu AJ, Johnson CH, Gonzalez FJ (2013) Targeted metabolomics of serum acylcarnitines evaluates hepatoprotective effect of Wuzhi tablet (Schisandra sphenanthera extract) against acute acetaminophen roxicity. Evid-Based Compl Alt 2013: 985257.

Chen C, Hennig GE, Manautou JE (2003) Hepatobiliary excretion of acetaminophen glutathione conjugate and its derivatives in transport-deficient (TR-) hyperbilirubinemic rats. Drug Metab Dispos 31: 798-804.

Choi YH, Lee HS, Chung CK, Kim EJ, Kang IJ (2017) Protective effects of an ethanol extract of *Angelica keiskei* against acetaminophen-induced hepatotoxicity in HepG2 and HepaRG cells. Nutr Res Pract 11: 97-104.

Ding Y, Li Q, Xu Y, Chen Y, Deng Y, Zhi F, Qian K (2016) Attenuating oxidative stress by paeonol protected against acetaminophen-induced hepatotoxicity in mice. PloS one 11: e0154375.

Du J, He D, Sun LN, Han T, Zhang H, Qin LP, Rahman K (2010) Semen Hoveniae extract protects against acute alcohol-induced liver injury in mice. Pharm Biol 48: 953-958.

Gonzalez-Ponce HA, Martinez-Saldana MC, Rincon-Sanchez AR, Sumaya-Martinez MT, Buist-Homan M, Faber KN, Moshage H, Jaramillo-Juarez F (2016) Hepatoprotective effect of Opuntia robusta and Opuntia streptacantha fruits against acetaminophen-induced acute liver damage. Nutrients 8: 607.

Huo Y, Yin S, Yan M, Win S, Aung Than T, Aghajan M, Hu H, Kaplowitz N (2017) Protective role of p53 in acetaminophen hepatotoxicity. Free Radical Biol Med 106: 111-117.

Hyun TK, Eom SH, Yu CY, Roitsch T (2010) *Hovenia dulcis*--an Asian traditional herb. Planta Med 76: 943-949.

Jiang Y, Fan X, Wang Y, Chen P, Zeng H, Tan H, Gonzalez FJ, Huang M, Bi H (2015) Schisandrol B protects against acetaminophen-induced hepatotoxicity by inhibition of CYP-mediated bioactivation and regulation of liver regeneration. Toxicol Sci 143: 107-115.

Kumari A, Kakkar P (2012) Lupeol prevents acetaminophen-induced in vivo hepatotoxicity by altering the Bax/Bcl-2 and oxidative stress-mediated mitochondrial signaling cascade. Life Sci 90: 561-570.

Larson AM, Polson J, Fontana RJ, Davern TJ, Lalani E, Hynan LS, Reisch JS, Schiodt FV, Ostapowicz G, Shakil AO, Lee WM, Acute Liver Failure Study G (2005) Acetaminophen-induced acute liver failure: results of a United States multicenter, prospective study. Hepatology 42: 1364-1372.

Lee HS, Lim WC, Lee SJ, Lee SH, Yu HJ, Lee JH, Cho HY (2016) Hepatoprotective effects of lactic acid-fermented garlic extract against acetaminophen-induced acute liver injury in rats. Food Sci Biotechnol 25: 867-873.

Li W, Yan MH, Liu Y, Liu Z, Wang Z, Chen C, Zhang J, Sun YS (2016) Ginsenoside Rg5 ameliorates cisplatin-induced nephrotoxicity in mice through inhibition of inflammation, oxidative dtress, and apoptosis. Nutrients 8: 566.

Liu LC, Wang CJ, Lee CC, Su SC, Chen HL, Hsu JD, Lee HJ (2010) Aqueous extract of Hibiscus sabdariffa L. decelerates acetaminophen-induced acute liver damage by reducing cell death and oxidative stress in mouse experimental models. J Sci Food Agr 90: 329-337.

Maieves HA, Ribani RH, Morales P, Sanchez-Mata MD (2015) Evolution of the nutritional composition of *Hovenia dulcis* Thunb. pseudofruit during the maturation process. Fruits 70: 181-187.

Ramachandran A, Jaeschke H (2017) Mechanisms of acetaminophen hepatotoxicity and their translation to the human pathophysiology. J Clin Transl Res 3: 157-169.

Reshi MS, Uthra C, Yadav D, Sharma S, Singh A, Sharma A, Jaswal A, Sinha N, Shrivastava S, Shukla S (2017) Silver nanoparticles protect acetaminophen induced acute hepatotoxicity: A biochemical and histopathological approach. Toxicol Pharmacol 90: 36-41.

Shanmugam S, Thangaraj P, Lima BDS, Chandran R, de Souza Araujo AA, Narain N, Serafini MR, Junior LJQ (2016) Effects of luteolin and quercetin 3-beta-d-glucoside identified from Passiflora subpeltata leaves against acetaminophen induced hepatotoxicity in rats. Biomed Pharmacother 83: 1278-1285.

Shih TY, Young TH, Lee HS, Hsieh CB, Hu OY (2013) Protective effects of kaempferol on isoniazid- and rifampicin-induced hepatotoxicity. AAPS J 15: 753-762.

Suke SG, Sherekar P, Kahale V, Patil S, Mundhada D, Nanoti VM (2018) Ameliorative effect of nanoencapsulated flavonoid against chlorpyrifos-induced hepatic oxidative damage and immunotoxicity in Wistar rats. J Biochem Mol Toxicol 32: e22050.

Tan Z, Luo M, Yang J, Cheng Y, Huang J, Lu C, Song D, Ye M, Dai M, Gonzalez FJ, Liu A, Guo B (2016) Chlorogenic acid inhibits cholestatic liver injury induced by alpha-naphthylisothiocyanate: involvement of STAT3 and NFkappaB signalling regulation. Pharm Pharmacol 68: 1203-1213.

Wang H, Fang ZZ, Meng R, Cao YF, Tanaka N, Krausz KW, Gonzalez FJ (2017) Glycyrrhizin and glycyrrhetinic acid inhibits alpha-naphthyl isothiocyanate-induced liver injury and bile acid cycle disruption. Toxicology 386: 133-142.

Wu H, Zhang G, Huang L, Pang H, Zhang N, Chen Y, Wang G (2017) Hepatoprotective effect of polyphenol-enriched fraction from Folium Microcos on oxidative stress and apoptosis in acetaminophen-induced liver injury in mice. Oxid Med Cell Longevity 2017: 3631565.

Xie WY, Jiang ZH, Wang J, Zhang XY, Melzig MF (2016a) Protective effect of hyperoside against acetaminophen (APAP) induced liver injury through enhancement of APAP clearance. Chem-Biol Interact 246: 11-19.

Xie WY, Wang M, Chen C, Zhang XY, Melzig MF (2016b) Hepatoprotective effect of isoquercitrin against acetaminophen-induced liver injury. Life Sci 152: 180-189.

Yan T, Wang H, Zhao M, Yagai T, Chai Y, Krausz KW, Xie C, Cheng X, Zhang J, Che Y, Li F, Wu Y, Brocker CN, Gonzalez FJ, Wang G, Hao H (2016) Glycyrrhizin protects against acetaminophen-induced acute liver injury via alleviating tumor necrosis factor alpha-mediated apoptosis. Drug Metab Dispos 44: 720-731.

Yang F, Tang X, Ding L, Zhou Y, Yang Q, Gong J, Wang G, Wang Z, Yang L (2016) Curcumin protects ANIT-induced cholestasis through signaling pathway of FXR-regulated bile acid and inflammation. Sci Rep 6: 33052.

Yoshioka H, Aoyagi Y, Fukuishi N, Gui MY, Jin YR, Li XW, Adachi Y, Ohno N, Takeya K, Hitotsuyanagi Y, Miura N, Nonogaki T (2017) Suppressive effect of kamebakaurin on acetaminophen-induced hepatotoxicity by inhibiting lipid peroxidation and inflammatory response in mice. Pharmacol Rep 69: 903-907.

Yuan J, Ge K, Mu J, Rong J, Zhang L, Wang B, Wan J, Xia G (2016) Ferulic acid attenuated acetaminophen-induced hepatotoxicity though down-regulating the cytochrome P 2E1 and inhibiting toll-like receptor 4 signaling-mediated inflammation in mice. Am J Transl Res 8: 4205-4214.